Available online at www.sciencedirect.com
SCIENCE DIRECT®
Catalysis Today 93–95 (2004) 567–574
CATALYSIS TODAY
www.elsevier.com/locate/cattod

Surface study of rhodium nanoparticles supported on alumina

A. Maroto-Valiente [a], I. Rodríguez-Ramos [a,*], A. Guerrero-Ruiz [b]

[a] *Instituto de Catálisis y Petroleoquímica, CSIC, Campus de Cantoblanco, 28049 Madrid, Spain*
[b] *Dpto. de Química Inorgánica y Técnica, UNED, Ciudad Universitaria, 28040 Madrid, Spain*

Available online 6 July 2004

Abstract

Two rhodium catalysts supported on alumina (metal loading 1 and 3 wt.%) were comparatively studied by H_2 and CO adsorption microcalorimetry and by infrared spectroscopy of the chemisorbed CO. The correlation of the results obtained from these two techniques with the *n*-butane hydrogenolysis reaction test provides useful information about the type and distribution of the surface active sites. The energetic distribution of surface sites has been shown to depend slightly on the metal loading and it can be modified by the pretreatment conditions. The obtained results also reveal the presence of partially reduced Rh atoms stabilized by Cl ions remaining from the precursor. On the other hand, the increased density on Rh (1 1 1) planes on the sample with 3 wt.% Rh treated with water, detected from CO adsorption experiments, can be related with enhanced both activity for the hydrogenolysis reaction and selectivity towards ethane.

Keywords: Supported metal catalysts; Alumina; CO adsorption; IR; Microcalorimetry; Butane hydrogenolysis

1. Introduction

Rhodium-containing catalysts have recently received particular attention due to their use in the three-way catalysts (TWC) for automotive emission control [1–4]. Also, this metal has been extensively applied in selective CO hydrogenation [5–9]. In general, catalytic performance of metal catalysts depends on the metal particle size (structure-sensitive reaction) and on the employed support [10,11]. However, to better understand the catalytic properties of rhodium catalysts, studies of their surface chemistry seem to be necessary in order to understand how the surface sites are modified, for instance by the pretreatment conditions. Among the many methods available, CO chemisorption followed by microcalorimetry and by infrared spectroscopy (IR) seems to be a very adequate approach. The former technique, calorimetry, can provide quantitative information about the energy of interaction of adsorbed molecules on catalyst surfaces, which is a parameter related with its surface structure [12–14]. While the latter (IR) can give useful information about the adsorption form of the CO probe molecule, and consequently the chemical state and active surface sites of the catalyst can be identified. In this work we have performed a surface analysis of supported Rh catalysts using adsorption calorimetry (H_2 and CO) and infrared spectroscopy of CO adsorption. Furthermore, the samples were evaluated in the *n*-butane hydrogenolysis reaction test. The final aim is to determine the nature of the surface sites on rhodium clusters supported on alumina, including aspects such as the presence of edge, corner or step atoms, or the type of exposed crystalline planes.

2. Experimental

2.1. Catalyst preparation

Al_2O_3 (Condea) with specific surface area of 220 m^2/g was used as support. This material was calcined in air at 973 K for 4 h prior to metal loading. The supported rhodium catalysts containing 1 and 3 wt.% of the metal were prepared by incipient impregnation of the support with aqueous solutions of $RhCl_3 \cdot H_2O$. After drying, the catalyst precursors were calcined in air at 773 K for 2 h. A portion of the calcined 3 wt.% metal loading sample was treated with steam at 773 K during 2 h. The water was fed into the re-

* Corresponding author. Tel.: +34 1 5854765; fax: +34 1 5854760.
E-mail address: irodriguez@icp.csic.es (I. Rodríguez-Ramos).

0920-5861/$ – see front matter © 2004 Elsevier B.V. All rights reserved.
doi:10.1016/j.cattod.2004.06.005

actor by bubbling a flow of helium (30 cm^3/min) through a saturator-condenser maintained at 293 K. The He/H_2O molar ratio was 98:2. The obtained samples were named 1RhAl, 3RhAl and 3RhAl-w (treated with water).

2.2. IR experiments

The Rh samples were pressed into self-supported wafers, ca. 10 mg/cm^2. An in situ glass made IR cell with CaF_2 windows was used for the IR experiments. The reduction treatments were carried out increasing the sample temperature, at 5 K/min, up to 673 (or 773 K) in a H_2 pulse (10^{-5} mol) and held at that temperature for 2 h. Then, the catalyst was outgassed at 673 K for 1 h. The IR spectra of reduced samples were recorded before and after exposure to 4 kPa of CO at room temperature. Subsequently, the IR spectra of 0the wafers were registered again after evacuated them with dynamic vacuum at 473 K for 1 h. All the spectra were collected using a Fourier transform infrared spectrometer (Nicolet 5 ZDX) equipped with a liquid nitrogen cooled MCT (mercury–cadmium–telluride) detector at a resolution of 4 cm^{-1} in the region 4000–1000 cm^{-1}. The results given herein are difference spectra with the spectrum of the clean sample before adsorption as the background.

2.3. Microcalorimetry measurements

The metallic dispersions and metal particle size were determined from the CO and H_2 chemisorption isotherms. These measurements were determined volumetrically with simultaneous measure of the evolved heats in each pulse by a Tian Calvet heat-flow calorimeter (Setaram C-80 II) operated isothermally at 330 K and connected to a glass vacuum-dosing apparatus. Doses of approximately 2×10^{17} molecules of the probe gas were introduced into the system to titrate the surface of metal catalysts. Both the calorimetric and volumetric data were stored and analyzed by microcomputer processing. The apparatus has been described in detail elsewhere [15]. For these experiments, the catalysts were first in situ reduced under hydrogen flow at 673 or 773 K for 2 h, outgassed overnight at the same temperature, and cooled to 330 K. The metal dispersion was obtained from the total amount of H_2 and CO uptake at the monolayer. This latter is considered to be covered when the evolved heat falls in the physisorption field (40 kJ/mol). The crystallite sizes were calculated from dispersion values using the equation d (nm) = 110/D [16].

2.4. Butane–H_2 reaction

The reaction studies have been performed in a glass tubular reactor, using 0.010–0.050 g of catalyst. The reaction was carried out at 463 K on reduced catalysts. The reactor was operated at atmospheric pressure and total conversions were kept low, below 15%. The reduction conditions were taken as 2 h at 673 or 773 K using a H_2 flow of about 40 cm^3/min. After reduction, the sample was cooled to the reaction temperature before introducing a flow of 99 cm^3/min of the H_2/n-C_4H_{10} mixture (10/1 ratio). The flow rates of these reactants were controlled by mass flow controllers (Brooks 5850 TR). The effluent gases were analyzed by gas chromatography (Varian, CP-3380) using a Porapak Q 80/100 column for products separation.

The catalytic activity per gram of rhodium was calculated from the following expression:

$$r = \frac{CF_{n\text{-}C_4H_{10}}}{100 W_{\text{rhodium}}} \frac{44.61}{60} \ (\mu\text{mol/g s})$$

where C is the percent of n-butane converted, $F_{n\text{-}C_4H_{10}}$ the flow rate (in cm^3/min) of n-butane through the reactor, and W the weight (in g) of the metal in the catalyst. Also, was calculated the activity per active center or turnover frequency (TOF) from the following expression:

$$\text{TOF} = \frac{r}{N_s} \ (s^{-1})$$

where N_s is the number of surface metal centers obtained from the hydrogen (TOF_H) and CO (TOF_{CO}) chemisorption measurements.

The following equation was used to calculate the selectivities for the production of ethane (S_E):

$$S_E = \frac{2C_2}{C_1 + 2C_2 + 3C_3} \times 100 \ (\%)$$

C_n values were calculated as mole percentage of products. The fragmentation factor of hydrogenolysis was defined as $\xi = \Sigma C_i/(\Sigma i C_i/4)$.

3. Results and discussion

Table 1 lists the metal dispersions and particle size determined by CO and H_2 chemisorption for the different alumina-supported rhodium catalysts. The metal dispersions were calculated by assuming M/H_2 = 2 and M/CO = 1 stoichiometries. It is seen that when both the temperature of reduction and the metal loading in the catalysts were increased changes were hardly observable in the total amount of H_2 and CO chemisorbed and therefore in the metal dispersion on 1RhAl and 3RhAl samples. Moreover, the values of the CO/H ratio are higher than 1 for all the samples. This circumstance is probably related to the formation of polycarbonylic species ($Rh(CO)_2$ or $Rh(CO)_3$ [17–19]). However, wet pretreatment at high temperature of the calcined 3 wt.% Rh sample caused a sharp drop in the H_2 and CO uptakes (Table 1). Moreover, this sample presents a lower CO/H ratio, which is close to 1. This finding may be explained by a change in the form of adsorption of CO molecule on the rhodium surface, i.e. the CO is adsorbed mainly in a linear mode.

Table 1
Surface properties of alumina-supported rhodium catalysts reduced at 673 and 773 K

Catalysts	%Rh	T_{Red} (K)	H_2 adsorption				CO adsorption				CO/H
			N_{ads} (μmol/g_{cat})	D (%)	d (nm)	q_0^{ads} (kJ/mol)	N_{ads} (μmol/g_{cat})	D (%)	d (nm)	q_0^{ads} (kJ/mol)	
1RhAl	1	673	22	45.3	2.4	130	70	72.0	1.5	175	1.59
		773	25	51.4	2.1	150	70	72.0	1.5	170	1.40
3RhAl	3	673	60	41.2	2.7	140	250	85.7	1.3	165	2.08
		773	80	54.9	2.0	160	245	84.0	1.3	170	1.53
3RhAl-w	3	673	36	24.7	4.4	120	84	28.8	3.8	175	1.17

3.1. H_2 adsorption

Table 1 and Figs. 1 and 2 show a comparison of the initial heats (q_0^{ads}) and microcalorimetric profiles of H_2 adsorption on the rhodium catalysts pretreated in different conditions. It is observed that the increase in the reduction temperature supposes a general enhancement of the heats of H_2 adsorption in practically the whole range of coverage. From the energetic point of view, the increase of reduction temperature induces the formation of surface sites of stronger adsorption for hydrogen on both catalysts (1RhAl and 3RhAl). The calorimetric curves for the samples 1RhAl and 3RhAl reduced at 673 K, and 1RhAl reduced at 773 K show one zone of constant value of differential adsorption heats around 70–90 kJ/mol. This plateau corresponds to H_2 coverage in the range 0.2–0.7 and indicates that a part of metal surface acts homogenously for the chemisorption of H_2. However, the sample 3RhAl reduced at 773 K shows a gradual decrease in the adsorption heat with the coverage (Fig. 1). This latter evidences a high heterogeneity in surface sites for H_2 adsorption. Moreover, this sample gives a total amount of chemisorbed H_2 slightly higher than the 3RhAl reduced at 673 K. This fact is contrary to that expected if metal particle sintering takes place upon reduction at higher temperature. It can be inferred that the increase in the reduction temperature produces probably some changes in the particle morphology and the generation of different adsorption centers. According with the literature [20–23], a more heterogeneous

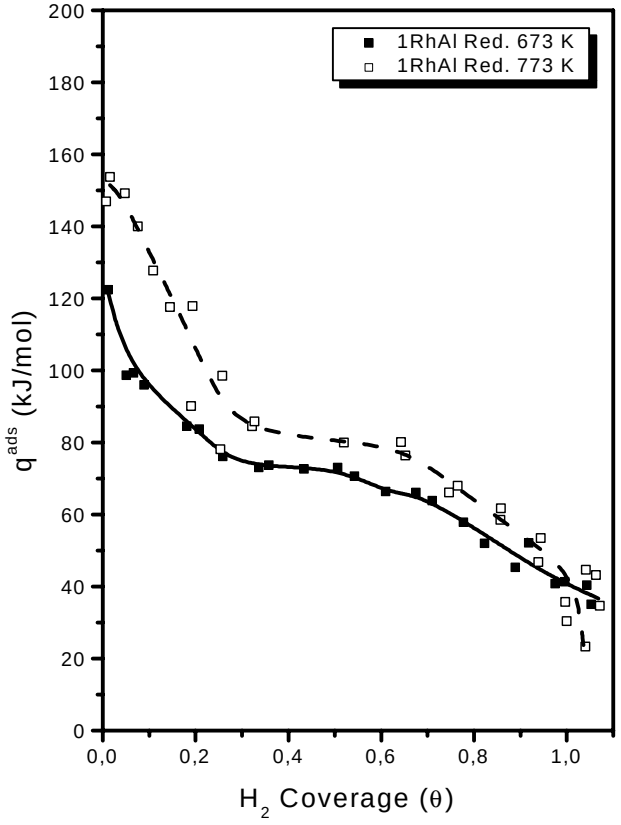

Fig. 1. Differential heats of H_2 adsorption at 330 K as a function of surface coverage for 1 wt.% Rh/Al_2O_3 catalysts.

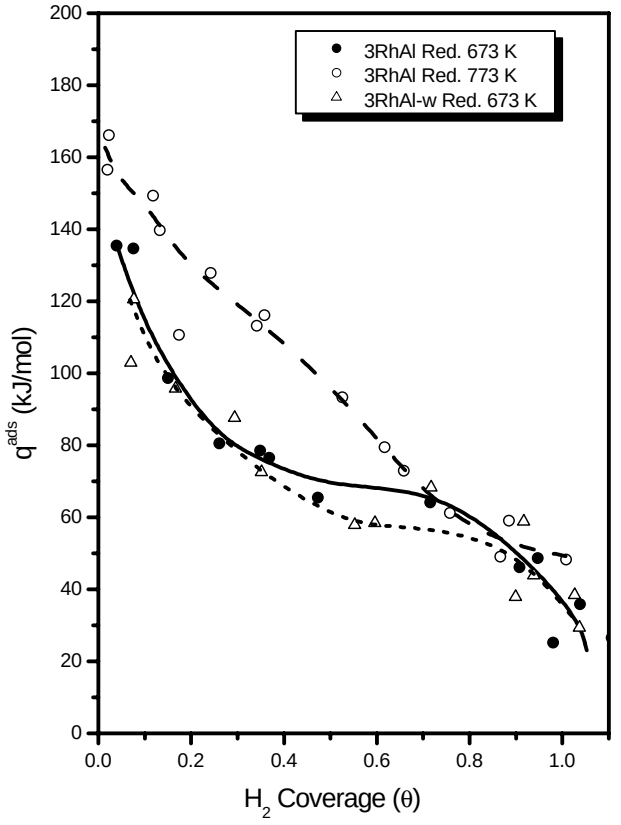

Fig. 2. Differential heats of H_2 adsorption at 330 K as a function of surface coverage for 3 wt.% Rh/Al_2O_3 catalysts.

distribution of surface sites for H_2 adsorption is produced by increasing the reduction temperature of the catalyst. On the other hand, when the calcined 3 wt.% Rh sample is treated in water vapor atmosphere (3RhAl-w) and then reduced at 673 K, the microcalorimetric profile is less affected. However, sintering of the rhodium particles is produced because a H_2 uptake lower than that of the 3RhAl reduced at 673 K is observed.

The initial heats of hydrogen adsorption obtained (120–160 kJ/mol) are higher than values reported in previous works for rhodium-supported catalysts [21,22] prepared from metallic precursors without chloride (85–117 kJ/mol). Crucq et al. [20,21] found for different Rh/Al_2O_3 catalysts prepared from $RhCl_3$ even higher values of q_0^{ads} (150–200 kJ/mol). The high values of hydrogen adsorption were explained as due to a slow adsorption of H_2 originated by the poisoning chlorine. In agreement with these authors, the microcalorimetry experiments of hydrogen adsorption over 1RhAl and 3RhAl catalysts suggest that these samples, which have been prepared with a chloride precursor, may still contain some Cl anions after reduction treatments. Probably the Cl anions occupy positions close to the Rh centers affecting their energy of interaction with hydrogen.

3.2. CO adsorption

The initial heats of CO adsorption collected in Table 1 are around 165–175 kJ/mol and scarcely change with the metal content and temperature reduction of the sample. These values are comprised between those previously reported for Rh/SiO_2, 160 kJ/mol [24], and for Rh/Al_2O_3, 190–195 kJ/mol [23,25]. On the other hand, these values are much higher than the obtained for Rh (1 1 1), approximately 134 kJ/mol [26]. Figs. 3 and 4 present the differential heats of CO adsorption on alumina-supported rhodium catalysts reduced at 673 and 773 K as a function of coverage. It can be seen for all the samples that the population of sites with such so high heat of adsorption is very small. The initial heat of adsorption sharply falls to values of adsorption heats at still low coverage significantly lower. The microcalorimetric profiles of 1RhAl samples (Fig. 3) exhibit one plateau with a stable value of differential heat of CO adsorption (115–120 kJ/mol) at low and medium coverage ($\theta = 0.05$–0.6). This quite constant value over a wide range indicates a homogeneous distribution of surface sites versus CO adsorption with respect to other surfaces. At higher coverage, in the case of the 1RhAl reduced at 673 K the adsorption heat decreases with further increase of the amount of CO chemisorbed to attain a value due to physisorption or reversible adsorption (ca. 40 kJ/mol) in the region of $\theta \sim 1$. However, when the 1RhAl sample is reduced at 773 K emerges a second plateau at CO coverage ($\theta = 0.6$–0.9) with a stable value of differential heat of adsorption (~95 kJ/mol) before falling to physisorption values. The 3RhAl sample reduced at 673 K shows a more heterogeneous CO adsorption behavior (Fig. 4), with a slow but continuous decay of differential heats from ca. 120 to 90 kJ/mol at CO coverage located between 0.1 and 0.9. Upon reduction at 773 K, two plateaus at coverages of $\theta = 0.1$–0.5 and 0.6–0.9, with heats of CO adsorption of 115 and 100 kJ mol^{-1}, are insinuated. Therefore, it appears that the surface present two populations of surface sites for CO adsorption in this coverage range. On the other hand, the 3RhAl-w sample reduced at 673 K displays two well differenced plateaus at coverages $\theta = 0.1$–0.5 and 0.6–0.8, with heats of CO adsorption ca. 125 and 95 kJ/mol, respectively. Clearly, three energetic different surface species are formed by CO adsorption on this 3RhAl-w catalyst, i.e., at very low coverage ($\theta < 0.1$, 175 kJ mol^{-1}), medium coverage ($\theta = 0.1$–0.5, 125 kJ/mol) and high coverage ($\theta = 0.6$–0.8, 95 kJ/mol).

Fig. 5 shows the infrared spectra of CO adsorbed on 1RhAl and 3RhAl treated at different conditions. When the catalysts were reduced at 673 K, four bands are observed at 1829 (very weak), 2065, 2030 and 2100 cm^{-1}. The IR bands observed at 2100 and 2030 cm^{-1} correspond, respectively, to the symmetric and antisymmetric ν_{CO} vibrations of *gem*-dicarbonyl species (Rh^+–$(CO)_2$) on small rhodium crystallites [17–19,25,27–36]. These bands are overlapped with the IR band of the linear species (Rh–CO, 2065 cm^{-1}) [18,25,27–30,34–36]. In addition, a broad IR band is detected at 1830–1850 cm^{-1} due to multibonded CO species

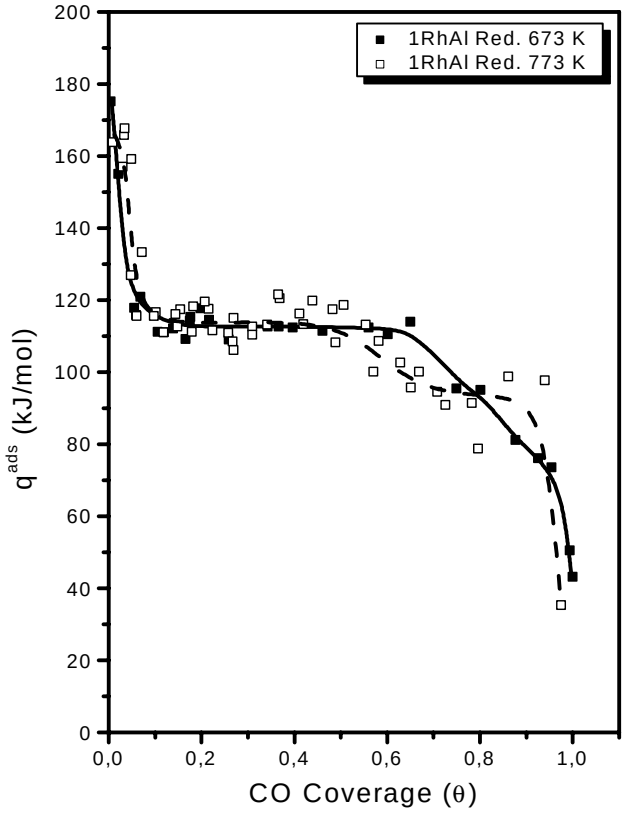

Fig. 3. Differential heats of CO adsorption at 330 K as a function of surface coverage for 1 wt.% Rh/Al_2O_3 catalysts.

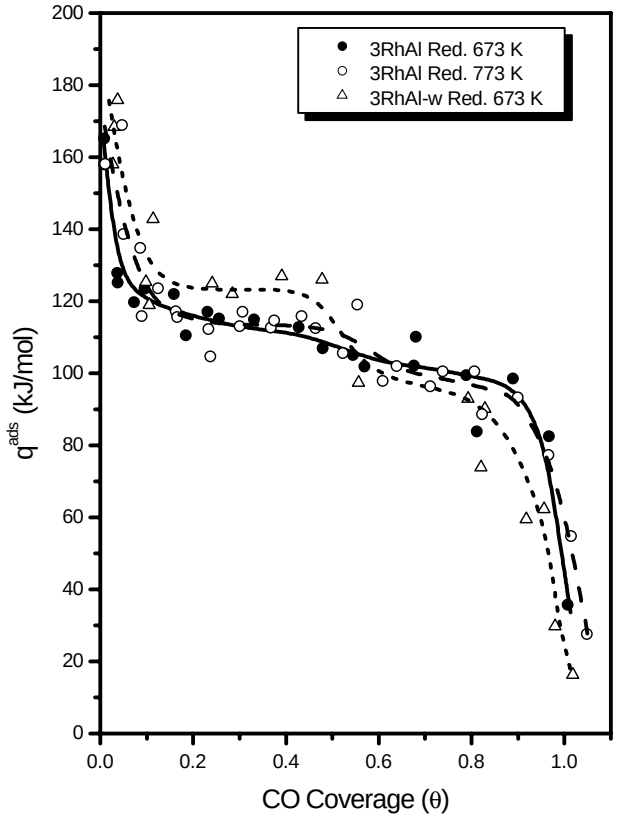

Fig. 4. Differential heats of CO adsorption at 330 K as a function of surface coverage for 3 wt.% Rh/Al_2O_3 catalysts.

(Rh_n–(CO), $n \geq 2$) [18,19,25,28,29,32–36]. The increase in the reduction temperature to 773 K supposes slightly for 1RhAl and in a major extent for 3RhAl catalyst an enhancement of the band stemming from linear CO (2065 cm^{-1}) with respect to the dicarbonyl species bands. Moreover, for 1RhAl sample the band attributed to linear CO species shifts to higher wavenumber and this band overlaps with the 2099 cm^{-1} from the symmetric ν_{CO} vibration of dicarbonyl species, resulting in a reversed relative intensity of the 2100 and 2031 cm^{-1} bands. This fact indicates a higher density of adsorbed CO species which results in a stronger dipolar coupling. The increase in the reduction temperature likely provokes the reduction in the roughness of the small particles in which a mixture of (1 1 1), (1 1 0), (1 0 0) and possibly other planes are exposed. This small particles evolve towards a morphology with higher crystallinity in which the high coordination (1 1 1) planes, mainly present in large particles, are more exposed. Since dicarbonyls species correspond to the dispersed phase and linear and multibonded CO to crystalline rhodium, from the IR spectra a growing number of larger clusters can be inferred when the reduction temperature is increased. This statement is specially consistent with the IR spectra of CO adsorbed on the 3RhAl-w sample reduced at 673 K where the band due to linearly adsorbed CO on Rh^0 predominates (Fig. 4). Data of CO chemisorption over 3RhAl-w (Table 1) confirm the diminution in the CO uptake with respect to the 3RhAl sample, probably derived from the sin-

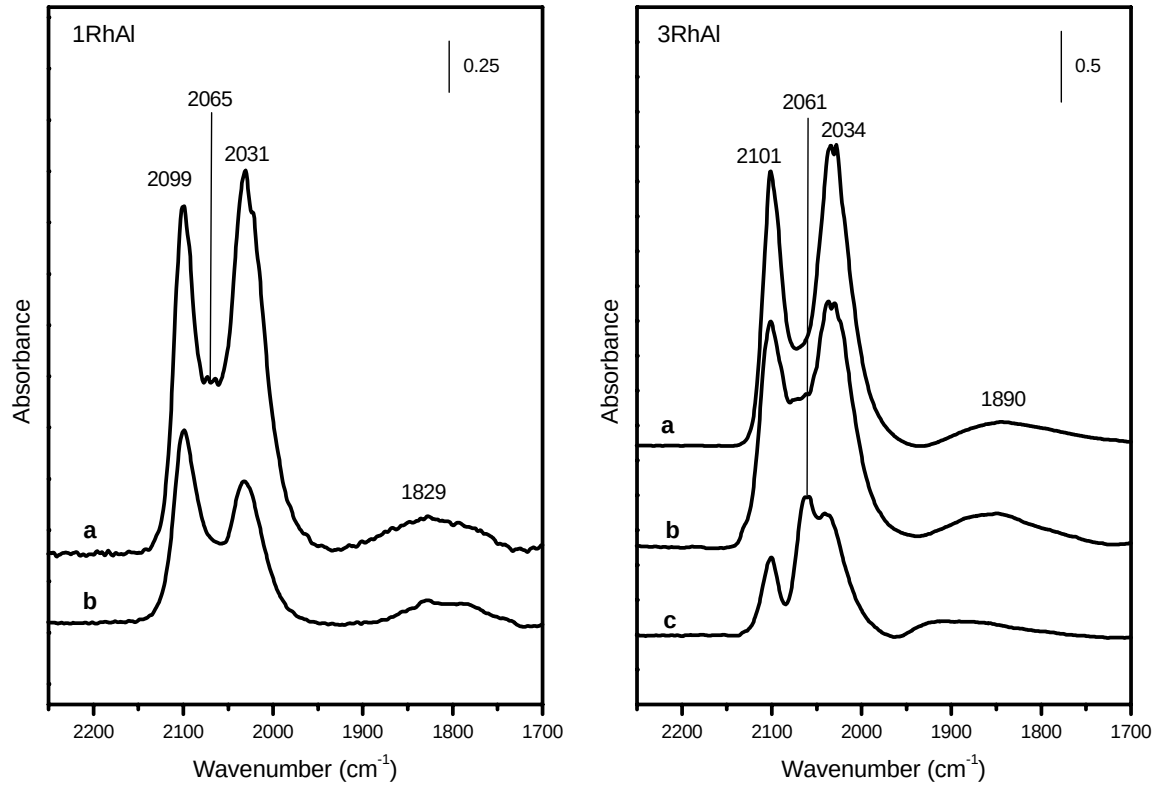

Fig. 5. IR spectra for CO adsorption on Rh/Al_2O_3 catalysts reduced at 673 K (a), reduced at 773 K (b) and pretreated in steam at 773 K and then reduced at 673 K (c).

tering of the rhodium particles. Moreover, the increase in reduction temperature to 773 K supposes for both 1RhAl and 3RhAl samples a widening of the peaks stemming from the *gem*-dicarbonyl species which suggest that the bands do not stem from a unique surface species but rater from slightly different species, most probably with slightly different geometrical configuration or/and bonded to different planes.

Based on the IR results of the CO adsorption (Fig. 5 and 6) the energy distribution showed by the calorimetric curves (Figs. 3 and 4) can be interpreted as follows. The initial adsorption heats showed in Table 1 which are in the very high-value range (165–175 kJ/mol) likely corresponds to the formation of multibonded CO species, since this species results in high adsorption strength of CO on Rh, and originates high initial adsorption heat. These values are similar to that obtained by Bianchi and coworkers [25] through spectroscopic methods for the CO adsorption on Rh/Al_2O_3. The differential adsorption heats in the medium-value region (140–115 kJ/mol) can be attributed to the formation of linearly adsorbed CO on Rh. Finally, adsorption heats in the low-value region (110–80 kJ/mol) can be ascribed to the formation of *gem*-dicarbonyl species on small Rh particles. Both multibonded and linear CO species are very scarce species on 1RhAl and 3RhAl samples reduced at 673 and 773 K, therefore adsorption heat drastically falls at very low coverage ($\theta < 0.2$) to the domain of low-value adsorption heats (110–80 kJ/mol), since dicarbonyl species are predominant on these samples. Moreover, the increase in the reduction temperature caused small differences in the adsorption heat values of the low-value region which indicate a slight modification in the surface site energy distribution. This latter being confirmed by small changes found in the IR spectra. After the 3RhAl catalyst is treated in water at 773 K sintering of the rhodium particles occurs; therefore the appearance of a plateau at medium adsorption heat values (125 kJ/mol), assigned to CO adsorption in a linear mode on larger clusters (Fig. 4), can be observed. The modification of the surface morphology varies the population of surface sites adsorbing CO in a specific mode and with a specific heat of adsorption, i.e., the linear species are enhanced while the *gem*-dicarbonyl species are reduced. The IR spectrum of CO adsorbed on 3RhAl-w (Fig. 5) clearly allows the assignation of the three zones of the CO adsorption heats showed in the calorimetric curve (Fig. 4) to the formation of multibonded, linear and *gem*-dicarbonyl adsorbed CO, respectively.

3.3. *n*-Butane reaction

Reaction of *n*-butane on these rhodium catalysts originates methane, ethane and propane, with neither production of isobutene by isomerization nor olefins by dehydrogenation. Data of catalytic activity, turnover frequency (TOF) and mole percentage of products (C_i) containing *i* carbon atoms are summarized in Table 2. Moreover, the deactivation of the catalysts, calculated by comparison of the activity at steady state with that obtained by extrapolation of the conversion versus time curve to time equal to zero, is given in this table. It is observed that the sample 3RhAl-w catalyst presents the highest value of turnover frequency (TOF_H) and also the lowest deactivation in reaction. The modification of the surface structure detected on 3RhAl-w sample with respect to 1RhAl and 3RhAl catalysts mainly caused by the sintering of the metal particles may be the origin of this behavior. Generally, changes of turnover frequency (TOF) for the hydrogenolysis of *n*-butane over rhodium-supported catalysts have been related with the variation of metallic particle sizes [37,38]. Kalakkad et al. [37] found that the catalytic activity increases with the increasing particle size on alumina-supported rhodium catalyst.

The distribution of various products in the *n*-butane hydrogenolysis for the different catalysts is shown in Table 2. It can be seen no significant changes in product distribution with the variation of the temperature reduction. Similar results were reported previously with rhodium-supported catalysts [37–43]. The values obtained for the fragmentation factor ($\xi \approx 2$) minimize the occurrence of the reaction via multibonded *n*-butane on three-fold or four-fold sites of rhodium planes, with the multiple split of the *n*-butane molecule. Therefore, single cleavage of the *n*-butane chain may take place through an adsorbed complex requiring only one surface Rh atom. It has been proposed that a metalacyclobutane is formed as intermediate on Rh metal [38,44]. The metalacyclobutane species can form $Rh(CH_2{=}CH{-}CH_3)(=CH_2)$ or $Rh(CH_2{=}CH_2)(=CH{-}CH_3)$ intermediates leading to the split of the terminal or the central C–C bond, respectively. Moreover, it has been found

Table 2
Catalytic properties of alumina-supported rhodium catalysts, for the *n*-butane/H_2 reaction at 463 K

Catalysts	T_{Red} (K)	d_H (nm)	Activity (μmol/g_{Rh} s)	TOF_H (10^{-3} s^{-1})	Deactivation (%)	Product distribution (%)			S_E (%)	ξ
						C_1	C_2	C_3		
1RhAl	673	2.4	33.2	7.5	98	31	50	19	53	2.1
	773	2.1	35.8	7.2	99	30	50	20	53	2.1
3RhAl	673	2.7	64.7	8.8	98	26	58	16	60	2.1
	773	2.0	33.9	9.3	96	27	57	16	60	2.1
3RhAl-w	673	4.4	77.9	32.5	72	20	63	17	65	2.0

that hydrogenolysis selectivity depends on the nature of the planes exposed by the Rh particles [43], the Rh(1 1 1) planes favoring the formation of Rh C_2-alkene, C_2-carbene species and therefore the ethane selectivity [38,43]. In Table 2 it is observed for the 1RhAl catalyst that the cleavage of the *n*-butane molecule corresponds nearly to the statistical value (50%). However, a rise in ethane selectivity (S_E) when the metal content is increased from 1RhAl to 3RhAl catalyst and majorly when the rhodium particles are sinterized by the water treatment, 3RhAl-w catalyst is observed. This is principally caused by changes of the surface structure, probably accompanied by the increase in the proportion of active centers that favors intermediates leading to central cleavage. This behavior is consistent with the changes in surface sites distribution found by IR and microcalorimetry of CO adsorption, and also with the known structure sensitivity of the alkane hydrogenolysis on rhodium [38].

4. Conclusions

The characterization by microcalorimetry of H_2 adsorption and CO adsorption, by IR of CO adsorbed and by the study of the *n*-butane reaction as probe of surface properties provided valuable information about alumina-supported rhodium catalysts, and the following points can be concluded.

1. The Rh catalysts evidence a heterogeneity of the surface sites for the adsorption of hydrogen. The increase in reduction temperature from 673 to 773 K contributes to strengthen the surface sites for hydrogen adsorption in the whole range of coverage.
2. The CO is adsorbed on rhodium catalysts in three different modes: multibonded, linear and *gem*-dicarbonyl species with differential heats of adsorption lying in the high (165–175 kJ/mol), medium (140–115 kJ/mol) and low (110–80 kJ/mol) field, respectively.
3. The surface morphology of the Rh catalysts, and as result, the fraction of sites adsorbing the CO in a specific mode, is influenced slightly by the reduction temperature and more specially by the pretreatment with water affect.
4. The *n*-butane hydrogenolysis over the Rh catalysts leads to single cleavage of the *n*-butane chain and it is a structure-sensitive reaction. On large particles the activity for this reaction is slightly increased and the central cleavage of *n*-butane becomes favored.

Acknowledgements

This work was supported by the Comunidad de Madrid under project 07M/0085/2002 and by the Spanish MCyT under project MAT 2002-04189-C02-01.

References

[1] K.C. Taylor, Catal. Rev.-Sci. Eng. 35 (1993) 457.
[2] P.J. Lévy, V. Pitchon, V. Perrichon, M. Primet, M. Chevrier, G. Gauthier, J. Catal. 178 (1998) 363.
[3] J. Barbier Jr., D. Duprez, Appl. Catal. B: Environ. 4 (1994) 105.
[4] D. Dulaurent, K. Chandes, C. Bouly, D. Bianchi, J. Catal. 192 (2000) 262.
[5] D.R. Watson, G.A. Somorjai, J. Catal. 72 (1981) 347.
[6] M.A. Vannice, J. Catal. 37 (1975) 449.
[7] G. Blyholder, L. Orji, Adsorpt. Sci. Technol. 4 (1987) 1.
[8] I. Mochida, N. Ikeyama, H. Ishibashi, H. Fujitsu, J. Catal. 110 (1988) 159.
[9] G. Van der Lee, B. Shuller, H. Post, T.L.F. Favre, V. Ponec, J. Catal. 98 (1986) 522.
[10] K. Hayek, R. Kramer, Z. Paal, Appl. Catal. A: Gen. 162 (1997) 1.
[11] P.L.J. Gunter, J.W. Niemantsverdriet, F.H. Ribero, G.A. Somorjai, Catal. Rev.-Sci. Eng. 39 (1997) 77.
[12] N. Cardona-Martinez, J.A. Dumesic, Adv. Catal. 38 (1992) 149.
[13] P.J. Anderson, H.H. Kung, Catalysis 11 (1994) 441.
[14] A. Guerrero-Ruiz, A. Maroto-Valiente, M. Cerro-Alarcón, B. Bachiller-Baeza, I. Rodríguez-Ramos, Topics Catal. 19 (2002) 311.
[15] B. Bachiller-Baeza, I. Rodriguez-Ramos, A. Guerrero-Ruiz, Langmuir 14 (1998) 3556.
[16] J.R. Anderson, Structure of Metallic Catalysts, Academic Press, New York, 1975, p. 295.
[17] H.P. Wang, J.T. Yates Jr., J. Catal. 89 (1984) 79.
[18] I. Mochida, N. Ikeyama, H. Ishibashi, H. Fujitsu, J. Catal. 110 (1988) 159.
[19] J.C. Conesa, M.T. Sainz, J. Soria, G. Munuera, V. Rives-Arnau, A. Muñoz, J. Mol. Catal. 17 (1982) 231.
[20] A. Crucq, L. Degols, A. Frennet, G. Lienard, Catal. Today 5 (1989) 223.
[21] A. Crucq, L. Degols, A. Frennet, G. Lienard, J. Mol. Catal. 59 (1990) 257.
[22] C. Force, A. Ruiz-Paniego, J.M. Guil, J.M. Gatica, C. López-Cortes, S. Bernal, J. Sanz, Langmuir 17 (2001) 2720.
[23] I. Toyoshima, G.A. Somorjai, Catal. Rev.-Sci. Eng. 19 (1979) 105.
[24] G.D. Zakumbaeva, L.A. Beketaeva, T.Yu. Uvaliev, A.S. Khlystov, A.Sh. Kuanyshev, Yu.M. Sagov, React. Kinet. Catal. Lett. 34 (1987) 213.
[25] O. Dulaurent, K. Chandes, C. Bouly, D. Bianchi, J. Catal. 192 (2000) 262.
[26] E.G. Seebauer, A.C.F. Kong, L.D. Schmidt, Appl. Surf. Sci. 31 (1988) 163.
[27] A.A. Efremov, N.I. Bakhmutova, Yu.D. Pankratiev, B.N. Kuznetsov, React. Kinet. Catal. Lett. 28 (1985) 103.
[28] M.N. Bredikhin, Yu.A. Lokhov, V.L. Kuznetsov, Kinet. Katal. 28 (1987) 558.
[29] G. Blyholder, L. Orji, Adsorpt. Sci. Technol. 4 (1987) 1.
[30] S.S.C. Chuang, C.-D. Tan, Catal. Today 35 (1997) 369.
[31] D.I. Kondarides, Z.L. Zhang, X.E. Verykios, J. Catal. 176 (1998) 536.
[32] P.J. Lévy, V. Pitchon, V. Perrichon, M. Primet, M. Chevrier, C. Gauthier, J. Catal. 178 (1998) 363.
[33] J. Raskó, J. Bontovics, Catal. Lett. 58 (1999) 27.
[34] P.B. Rasband, W.C. Hecker, J. Catal. 139 (1993) 551.
[35] Z.L. Zhang, A. Kladi, X.E. Verykios, J. Mol. Catal. 89 (1994) 229.
[36] D.J.C. Yates, L.L. Murrel, E.B. Prestidge, J. Catal. 57 (1979) 41.
[37] D. Kalakkad, S.L. Anderson, A.K. Datye, Stud. Surf. Sci. Catal. 75 (1991) 2411.
[38] D. Kalakkad, S.L. Anderson, A.D. Logan, J. Peña, E.J. Braunschweig, C.H.F. Peden, A.K. Datye, J. Phys. Chem. 97 (1993) 1437.

[39] S. Gao, L.D. Schmidt, J. Catal. 111 (1988) 210.
[40] M.J. Holgado, A.C. Iñigo, V. Rives, React. Kinet. Catal. Lett. 54 (1995) 297.
[41] M.J. Holgado, A.C. Iñigo, V. Rives, Appl. Catal. A: Gen. 175 (1998) 33.
[42] J.J. Calvino, M.A. Cauqui, G. Cifredo, J.M. Rodriguez-Izquierdo, H. Vidal, J. Sol-Gel Sci. Technol. 2 (1994) 831.
[43] H. Vidal, S. Bernal, R.T. Baker, G.A. Cifredo, D. Finol, J.M. Rodríguez-Izquierdo, Appl. Catal. A: Gen. 208 (2001) 111.
[44] P.L. Dhepe, A. Fukuoka, Ichikawa, Catal. Lett. 81 (2002) 69.